ECOLOGY LETTERS

Ecology Letters, (2013) **16**: 1069–1078 doi: 10.1111/ele.12127

LETTER

An empirical assessment of tree branching networks and implications for plant allometric scaling models

Lisa Patrick Bentley,[1]* James C. Stegen,[2] Van M. Savage,[3,4,5] Duncan D. Smith,[6] Erica I. von Allmen,[6] John S. Sperry,[6] Peter B. Reich[7,8] and Brian J. Enquist[1,4]

Abstract

Several theories predict whole-tree function on the basis of allometric scaling relationships assumed to emerge from traits of branching networks. To test this key assumption, and more generally, to explore patterns of external architecture within and across trees, we measure branch traits (radii/lengths) and calculate scaling exponents from five functionally divergent species. Consistent with leading theories, including metabolic scaling theory, branching is area preserving and statistically self-similar within trees. However, differences among scaling exponents calculated at node- and whole-tree levels challenge the assumption of an optimised, symmetrically branching tree. Furthermore, scaling exponents estimated for branch length change across branching orders, and exponents for scaling metabolic rate with plant size (or number of terminal tips) significantly differ from theoretical predictions. These findings, along with variability in the scaling of branch radii being less than for branch lengths, suggest extending current scaling theories to include asymmetrical branching and differential selective pressures in plant architectures.

Keywords

Allometry, hierarchical Bayesian, metabolic scaling theory, network topology, plant traits, WBE model.

Ecology Letters (2013) **16**: 1069–1078

INTRODUCTION

The study of plant architecture has led to two dominant viewpoints about evolutionary and biophysical origins of plant branching patterns. On one hand, diversity in plant architecture has been categorised according to differences in individual-level selection across growth environments that help determine taxon-specific allocation and life history (Callaway *et al.* 1994; Ackerly & Donoghue 1998). A variety of architectural branching designs exist in nature (Hallé *et al.* 1978) and differences in architecture are often matched by specific genes that regulate growth and development (Wang & Li 2006; Bosch *et al.* 2008). On the other hand, studies of plant architecture have sometimes focused on similarities in the patterns of branching (Shinozaki *et al.* 1964; Horn 2000; Eloy 2011) as measured by the scaling of branch dimensions, such as number, radius, and length (McMahon & Kronauer 1976; West *et al.* 1997, 1999; Olson *et al.* 2009).

In light of these viewpoints, researchers have constructed network models that assume general architectural principles that underlie tree branching structure and can be used to predict scaling of plant form and function within and across taxa. The insight of this approach arises because structure and geometry of branches and roots directly affect light, water and nutrient capture (Cannell 1989; Küppers 1989), as well as mechanical support (Rosell *et al.* 2012), reproduction (Archibald & Bond 2003; Leslie 2012), and competitive ability (Pretzsch & Dieler 2012). However, this approach to describing plant structure ignores variation in branching traits both within and/or across species (e.g. West *et al.* 1997, 1999). In essence, these plant-scaling models assume mean values of branching traits characterise branching network architecture or geometry provides a mechanistic basis to scale physiological processes (e.g. metabolic rate) with plant size (e.g. mass). These relationships are reflected in simple size-based scaling relationships that are posited to arise due to evolutionary optimisation principles (West *et al.* 1997, 1999; Vasseur *et al.* 2012).

Despite the importance of coupling tree branching architecture (form) with physiological function to predict whole-tree and canopy-level processes (West *et al.* 2009; Stegen *et al.* 2011; Feng *et al.* 2012; Makela 2012), few studies have assessed external branching patterns at the level of the branch node or the whole tree and analysed data in the context of plant-scaling models (Shinozaki *et al.* 1964; Leopold 1971; Barker *et al.* 1973; McMahon & Kronauer 1976; Bertram 1989; Horn 2000; Sone *et al.* 2005; Dahle & Grabosky 2010; Costes & Guedon 2012). To characterise both similarities and differences in branching structure within and across species, we deconstructed branching networks of nine trees from five functionally divergent species and measured branching dimensions for all branches at both branch- and whole-tree levels.

We also used our unique data set to directly test several assumptions and predictions of the West, Brown, and Enquist (WBE) plant-scaling model (West *et al.* 1997, 1999). The WBE model derives branching rules using the principle that energy is minimised

[1]*Department of Ecology and Evolutionary Biology, University of Arizona, Tucson, AZ, 85721, USA*
[2]*Fundamental and Computational Sciences, Biological Sciences, Pacific Northwest National Laboratory, Richland, WA, 99352, USA*
[3]*Department of Biomathematics, University of California at Los Angeles, David Geffen School of Medicine, Los Angeles, CA, 90095, USA*
[4]*Santa Fe Institute, Santa Fe, NM, 87501, USA*
[5]*Department of Ecology and Evolutionary Biology, University of California at Los Angeles, Los Angeles, CA, 90095, USA*
[6]*Department of Biology, University of Utah, Salt Lake City, UT, 84112, USA*
[7]*Department of Forest Resources, University of Minnesota, Saint Paul, MN, 55108, USA*
[8]*Hawkesbury Institute for the Environment, University of Western Sydney, Locked Bag 1797, Penrith, NSW, 2751, Australia*
**Correspondence: E-mail: lpatrick@email.arizona.edu*

for the flow of water and nutrients from trunk to petioles along with a particular form of space filling that matches the sum of the service volumes (three-dimensional spheres with diameter proportional to branch length) across branching orders. Together, these principles maximise scaling of resource uptake and delivery at each level. A detailed description of the WBE model as it relates to this paper is presented in Fig. 1 and Table 1 with additional details in Table S1 and Appendix S1. Importantly, the WBE model also assumes the branching is symmetrical – that is, at each branching node, all daughter branches have *identical* lengths and radii. These assumptions can be used to derive that the branching network is self-similar (e.g. fractal). Because real trees exhibit asymmetric branching of various degrees, our best test of the WBE model is to determine how well the theory based on an optimised, symmetrically branching tree (with the average node-level branching properties of a real tree) does at predicting whole-plant allometric scaling. Because our approximate tests of metabolic scaling theory's assumptions and predictions use directly measured branch dimensions to calculate branch-level scaling properties, our tests go beyond past indirect tests based only on whole-tree measurements (Price *et al.* 2009, 2012a). These direct tests are critical because WBE model extensions build upon these external branching principles (Enquist *et al.* 2007, 2009; West *et al.* 2009) and predict that whole-plant carbon and water fluxes, net primary production, and population density should be characterised by similar scaling functions.

METHODS

Study species and data collection

We created what is to our knowledge the largest data set yet assembled on node-specific architecture of entire tree branching networks. We sampled individuals of five tree species that broadly differ in terms of their external architecture (e.g. varying levels of apical dominance and apical control), evolutionary history (e.g. angiosperm vs. gymnosperm), xylem vascular anatomy (e.g. diffuse porous vs. ring porous) and growing environment (e.g. temperate vs. tropical). We sampled three angiosperm trees: one *Acer grandidentatum* (Sapindaceae; bigtooth maple; 17-year old) and one *Quercus gambelii* (Fagaceae; Gambel oak; 4-year old) from Red Butte Canyon Natural Research Area in Salt Lake County, Utah; and one mature *Ochroma pyramidale* (Malvaceae; balsa; 20- to 40-year old) from secondary forest in the Rincon National Park, Guanacaste, Costa Rica. The *Q. gambelii* and *A. grandidentatum* are the identical trees used in von Allmen *et al.* (2012). In addition, we sampled six gymnosperm trees, including one *Pinus edulis* (Pinaceae; piñon pine; 23-year old) from a ranch near Ojitos Frios, NM; and five *Pinus ponderosa* (Pinaceae; ponderosa pine, range from 2 to 5-year old) collected from Mt. Lemmon in Coronado National Forest, Arizona. All measured trees were open-grown and dominant or co-dominant in their respective ecosystems. Selected trees were from undisturbed areas and relatively isolated from other trees in the study areas. As such, we assume that each tree is not strongly resource limited. We recognise that these tree canopies could have been influenced by competition for resources (i.e. light) that might cause the architecture of these trees to deviate from either a symmetrical or fractal ideal (Pretzsch & Dieler 2012).

After all trees were harvested, we identified, counted and labelled *all* branching points (nodes) and branches (internodes). Measurements were made of branch diameter (distal and proximal) and branch length. Data were collected for all nodes throughout each tree except balsa due to time and logistical constraints. In total, our data set includes empirical measurements for approximately 7100 branching nodes.

Calculating WBE scaling exponents

In the context of WBE, a tree's external architecture is defined by branching furcation numbers, branch diameters and branch lengths (Fig. 1, Table 1). Through additional assumptions and the prediction that branching dimensions are self-similar across branching nodes, these branch-level attributes can further predict scaling of

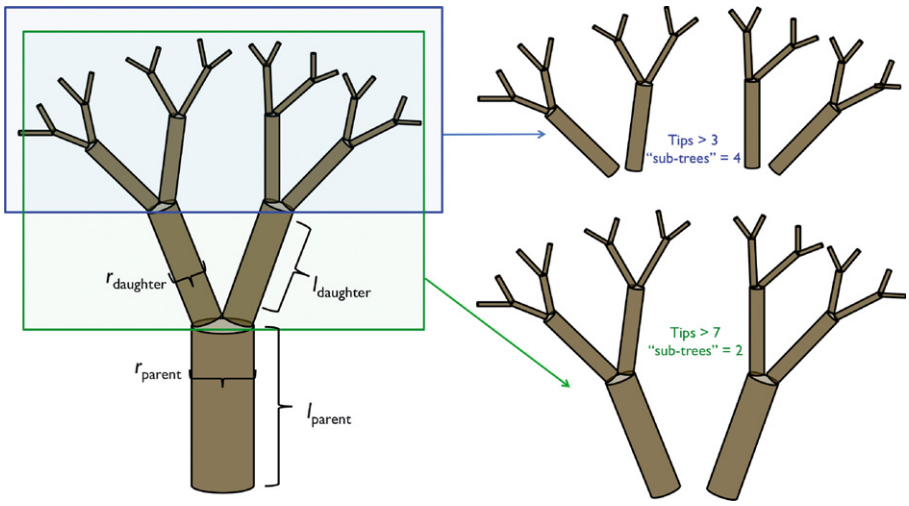

Figure 1 Although the WBE model predicts scaling exponents related to both internal (vascular) and external (branching) networks, here we were interested in testing assumptions and predictions only related to the scaling of external tree geometries (see Tables 1 and S1). Within the WBE model, it is assumed that the tree's external branching network is a symmetrical, self-similar and hierarchical branching network. As such, values for scaling exponents as defined by the WBE model (e.g. a and b) should not vary throughout the tree and should be identical at both the branch and whole-tree levels (e.g. $a_{node} = a_{tree} = a$ and $b_{node} = b_{tree} = b$). Since these assumptions imply that a small piece of the network is representative of the whole network, we were able to use a subsetting method to estimate whole-tree scaling exponents.

Table 1 Scaling exponents calculated at both the branch-level (across nodes) and whole-tree level (across 'sub-trees') using architecture-based measurements. Note that at both the branch and whole-tree levels, scaling exponents for branch length and radii can only be used to calculate the scaling of estimated metabolic rate in the limit for networks of infinite size and with no pathlength effect on hydraulics. Furthermore, all whole-tree equations relate tree volume to the number of leaves per tree, assume invariance in leaf traits, and can be related to each other through their exponents (i.e. a_{tree} and b_{tree} are allowed to co-vary and the value for θ_{tree} is informed by distributions for a_{tree} and b_{tree}). Additional details and assumptions related to these exponents within the context of the WBE model are provided in Appendix S1. Definitions are as follows: r = branch radii, n = number of branches, r_0 = the measured radius at the tree's base, N_N = the total number of terminal branches, l = branch length (distance between branching nodes), l_{TOT} = the tree's pathlength that corresponds to the continuous column of water travelling from the tree's base to the most distant terminal branch, V = volume (related to mass via density) of all branches of the whole tree (including the main stem), s = branch segment and Ns = total number of branch segments per tree

Exponent		Level	Equation
a	Radius scaling	Branch (node)	$a_{node} = -\frac{\ln \beta_{node}}{\ln n_{node}}$, where $\beta_{node} = \frac{r_{daughter}}{r_{parent}}$, $n_{node} = \frac{n_{daughter}}{n_{parent}}$
		Whole tree	$N_N \propto r_0^{\frac{1}{a_{tree}}}$
b	Length scaling	Branch (node)	$b_{node} = -\frac{\ln \gamma_{node}}{\ln n_{node}}$, where $\gamma_{node} = \frac{l_{daughter}}{l_{parent}}$
		Whole tree	$N_N \propto l_{TOT}^{\frac{1}{b_{tree}}}$
θ	Estimated metabolic rate	Branch (node)	$\theta_{node} = \frac{1}{2a_{node} + b_{node}}$
		Whole tree	$N_N \propto V^{\theta_{tree}}$, where $V = \sum_{s=1}^{Ns} \pi r_s^2 l_s$

whole-tree metabolic rate (Appendix S1). Here, we used two methods to estimate branch radii and branch length exponents (a and b respectively) and calculate the estimated metabolic rate scaling exponent (θ) based on branching architecture.

METHOD 1: RATIO-BASED APPROACH FOR BRANCH-LEVEL SCALING EXPONENTS

To calculate WBE scaling exponents at the branch-level, we used the statistical platform 'R' (R Development Core Team 2012) to calculate branching ratios, radii ratios and length ratios for each node (Table 1). We then calculated radii and length scaling exponents at each node (a_{node} and b_{node} respectively) from measures of branch radii and lengths of mother and daughter branch segments (Fig. 1, Table 1). Because daughter branches at a given node were not identical, ratios for each node were calculated for each daughter branch (e.g. a node with five daughter branches would have five calculated radii ratios and five length ratios). Scaling exponents a_{node} and b_{node} from each daughter-to-parent pairing were then used to calculate node-level estimated metabolic rate scaling exponent, θ_{node} (Table 1). We emphasise this method does not explicitly measure metabolic rate, but rather, uses assumptions based on space filling and elastic similarity to estimate the exponent of how metabolic rate scales with plant size from branching traits (Appendix S1). As such, we refer to this rate always as 'estimated metabolic rate' or this exponent as 'estimated metabolic rate exponent'. Lastly, we used the median of these exponents across all branch nodes within a tree ($\bar{a}_{node}$, $\bar{b}_{node}$ and $\bar{\theta}_{node}$) to provide branch-level estimates of scaling of branch lengths, branch radii and estimated metabolic rate at a whole-tree level. We did not use an arithmetic mean since we did not want to assume unimodal and roughly symmetrical distributions and we could not use a geometric mean due to negative numbers. Importantly, branch-level exponents were always calculated using raw data from real trees and then averaged. Data from sub-sampled trees (see below) were not used for this method.

METHOD 2: REGRESSION-BASED APPROACH FOR WHOLE-TREE SCALING EXPONENTS

Using individual branch radii and length measurements, we calculated number of terminal branches (N_N), total branch volume (V) and maximum pathlength (l_{TOT}) for each measured tree. We then sub-sampled branches within each tree to create a large data set with enough size variation to estimate whole-tree level scaling exponents related to branch radii, branch lengths and estimated metabolic rate (a_{tree}, b_{tree} and θ_{tree} respectively). This was done because WBE predicts the same results for both whole and sub-sampled trees, and because it increases the total number of estimated scaling exponents, which was needed because only one whole tree was sampled per species (except for ponderosa pine, where five trees were sampled). We used an iterative process to create subsets of each tree's full branching network (Fig. 1). For this analysis, branches were systematically removed starting from the base of the branching network. With each iteration, we produced a smaller subset of networks that were nested within larger subsets of networks from previous iterations. This procedure resulted in a large number of network subsets that varied greatly in their size (i.e. the total number of branches). Each subset was considered a complete network such that N_N, V, the measured base radius (r_0), and l_{TOT} were calculated for each network. Sample sizes of the number of 'sub-trees' included in each binned subset are listed in Fig. 5. See Appendix S2 for more details related to Method 2.

Subsets of a single tree are not independent samples and are not representative of how architecture changes as a tree gets larger (e.g. how growth changes in response to shading or crowding), but examining ontogenetic branching patterns was not our goal. Rather, we focused on examining snapshots of tree architecture in time, and as such, this subsetting method is appropriate since we were testing our data within the context of self-similar, fractal-like networks as defined by WBE wherein a small piece of the network is representative of the whole network. Importantly, as shown in Fig. S1 and discussed in the results, WBE network scaling exponents do not change systematically with parent diameter using this method.

After creating tree subsets (hereafter referred to as 'sub-trees'), we used standardised major axis (SMA) regression (Warton *et al.* 2006) to simultaneously estimate a_{tree}, b_{tree} and θ_{tree} within a hierarchical Bayesian (HB) framework similar to Price *et al.* (2009; see Appendix S3 for a detailed explanation of the model, code and implementation

procedures). Using this method, a_{tree} and b_{tree} are allowed to co-vary, and the value for θ_{tree} is informed by distributions for a_{tree} and b_{tree}. Compared to a frequentist regression approach, we are better able to estimate scaling exponents using the HB framework because it allows us to explicitly account for measurement error (in branch radius), allows for the possibility that observation (and process) errors associated with the other variables (l_{TOT}, V and N_N) are correlated, and accounts for variability between trees and species. We implemented our models in OpenBUGS (Lunn *et al.* 2000), a general-purpose statistical software package for conducting Bayesian analyses.

Testing and evaluating WBE assumptions and predictions

At both the branch- and whole-tree levels, scaling exponents are assumed to be interdependent and as such determine how numerous allometric relationships covary with each other (Price *et al.* 2007; Price & Weitz 2012). An alternative model is that allometric scaling relationships instead are governed by other processes *not* related to these particular values for the average scaling of branching traits. Indeed, whole-tree scaling exponents can be estimated independently by relaxing *all* of the WBE constraints and assumptions related to branching architecture of a symmetrical, optimised tree (SPAM model in Price *et al.* 2009). Simply put, whole-tree exponents for the scaling of length, radii and estimated metabolic rate (a_{tree}, b_{tree}, θ_{tree}) can also be estimated outside the context of the WBE model as empirically fitted slopes. For instance, $1/a_{tree}$, $1/b_{tree}$, θ_{tree} simply become x, y, z coordinates in a space of possible symmetrically branching tree geometries, and each coordinate can be determined from fits using Method 2. Thus, within our HB model framework, we estimated both WBE predicted and empirically fitted scaling exponents (e.g. SPAM model exponents as in Price *et al.* 2009) at the whole-tree level; if both the WBE predicted and SPAM fitted scaling exponents at the whole-tree level overlap, then we conclude that WBE assumptions regarding interdependence of branching traits are appropriate for real trees (or in cases where the empirical values have large uncertainty, are at the very least not inconsistent). For example, since WBE estimates for the scaling of volume do not vary independently of the scaling of branch length and radii (e.g. θ_{tree} draws on the estimated distributions of a_{tree} and b_{tree}), overlap of WBE and SPAM estimates for θ suggests that a_{tree} and b_{tree} likely do determine θ_{tree}. We refer to the SPAM estimated exponents by the notational conventions of the WBE model (a_{SPAM}, b_{SPAM} and θ_{SPAM}) for convenience in comparison only.

We also evaluate core and secondary assumptions of the WBE model using both branch- and whole-tree scaling exponents. These analyses are summarised in Table S1 and a detailed background on their origins within the WBE framework are presented in Appendix S1. It is important that our regression models assumed symmetrical branching that we characterise with average power-law functions across branching orders. See Appendix S4 for more details.

RESULTS

Do WBE and SPAM estimated scaling exponents overlap?

Across all species, using Method 2, estimates using the SPAM model for whole-tree scaling of branch radii (a_{SPAM} = 0.593–0.652, range across subsets) and lengths (b_{SPAM} = 0.533–0.833, range across subsets) were larger than WBE estimates (a_{tree} = 0.550–0.591 and b_{tree} = 0.467–0.777, range across all subsets) based on a symmetrically branching tree, but were not significantly different within or across species due to overlap of 95% CIs (Fig. S5, Table S3). Estimated metabolic rate scaling exponents at the whole-tree level were also not significantly different between WBE (θ_{tree} = 0.533–0.623) and SPAM (θ_{SPAM} = 0.534–0.634, range across subsets) models due to overlap of 95% CIs (Fig. S5, Table S3).

Testing additional WBE model assumptions and predictions

Do branch-level measurements 'scale up' to predict whole-tree exponents both within and across species?

To determine if observed branch-level relationships were representative of whole-tree allometric scaling patterns, we compared median *intra*specific scaling exponent estimates from both Method 1 ($\bar{a}_{node}$, $\bar{b}_{node}$ and $\bar{\theta}_{node}$) and Method 2 (a_{tree}, b_{tree}, and θ_{tree}) (Fig. 2). As

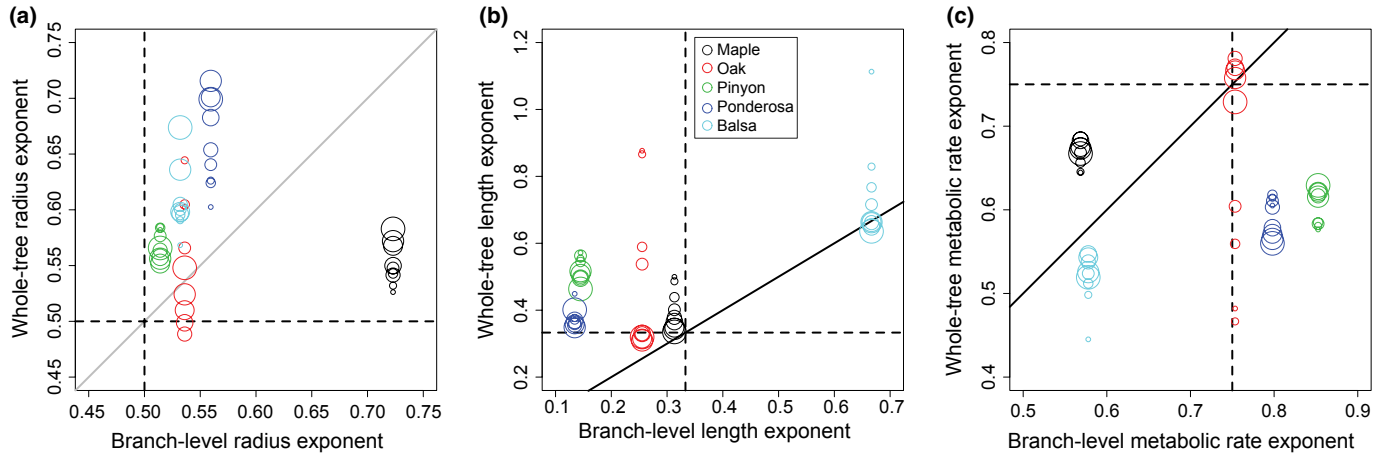

Figure 2 A comparison of branch-level (ratio-based) and whole-tree (hierarchical Bayesian regression-based) median scaling exponents for (a) radius, (b) length and (c) architecture-based metabolic rate for all trees. The solid line is the 1 : 1 line and the dashed lines indicate the WBE model prediction for an allometrically optimised tree. Different sized circles indicate different whole-tree data sets used for analyses, where smaller circles indicate data sets that include subsets of 'sub-trees' with a smaller number of minimum terminal tips included and larger circles indicate data sets that include subsets of 'sub-trees' with a larger number of terminal tips included.

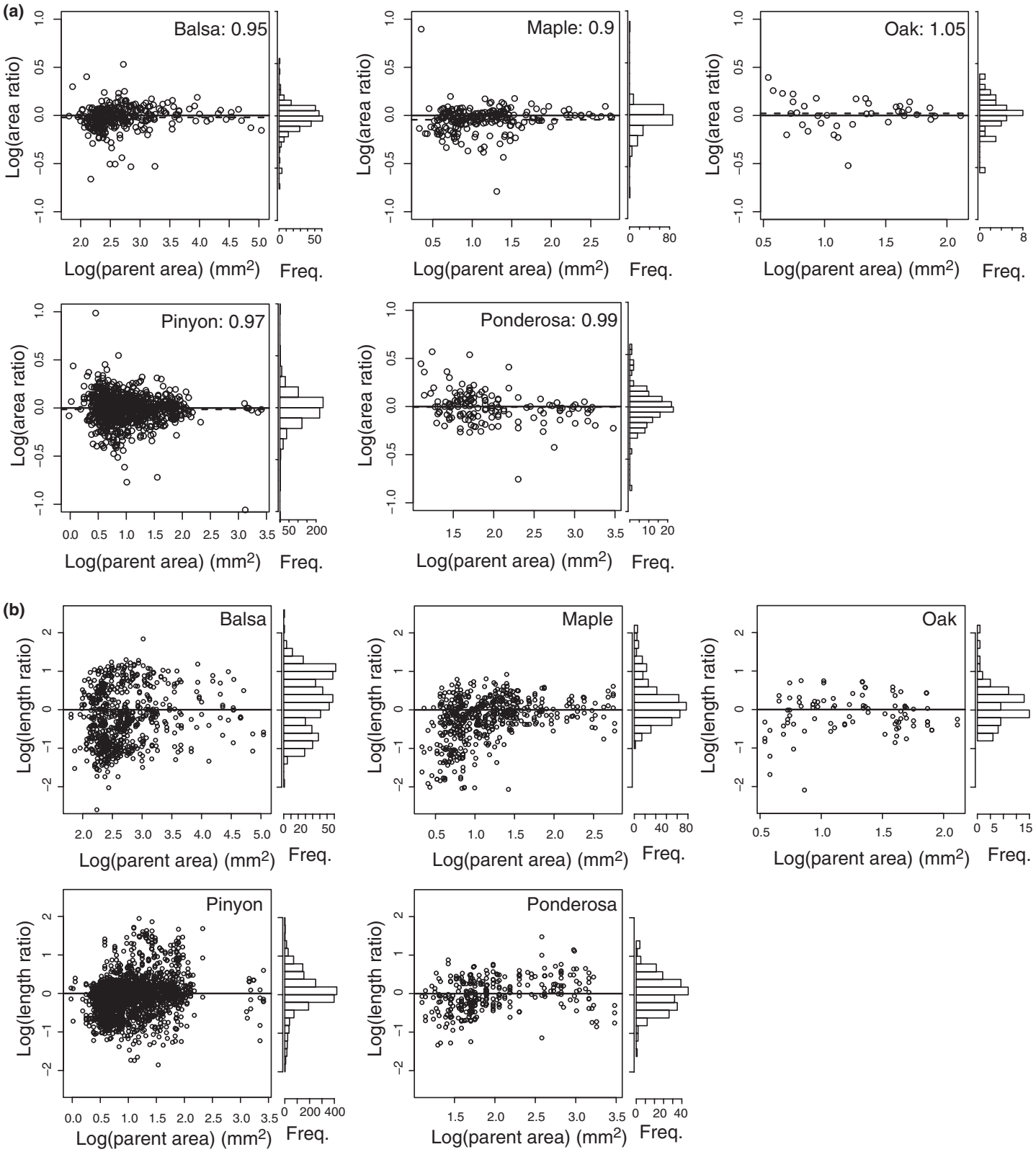

Figure 3 (a) The ratio of the sum of daughter branch area to the single parent branch area versus parent branch area in all five species measured. The horizontal solid line at unity indicates area preservation and the dashed horizontal line indicates the mean of the empirical data. The empirical means are also listed next to tree names. (b) Ratio of daughter branch length to parent branch length versus parent branch area in all five species measured. Panel b is included to allow for a "common" x axis for comparing variation in area scaling (panel a) and length scaling.

previously mentioned, the median was used due to the presence of extreme values and asymmetrical distributions at the branch-level (Table S4). Since values for all data sets across species did not overlap with the 1 : 1 line, our results indicate that for the trees measured, branch-level estimates of scaling exponents do not provide reliable estimates of those same exponents for whole trees (Fig. 2). However, since the estimation of θ_{tree} in the HB model for WBE is constrained by the distributions of a_{tree} and b_{tree}, overlap of WBE and SPAM values for the estimated metabolic rate scaling exponent does indicate that branching exponents are indeed connected to the branching geometry of whole-tree network (Fig. S5, Table S3).

Do trees exhibit area-preserving branching? What is the corresponding scaling exponent for a symmetrically branching, self-similar tree?

Intraspecific patterns. Area-preserving branching was demonstrated since the total cross-sectional area of daughter branches was approximately equal to that of their parent's cross-sectional area for all species (Fig. 3). For all species (maple, oak, piñon, ponderosa, balsa), the observed branch-level values of a_{node} [estimate (95% CI)] for individual trees [a_{node} = 0.72 (0.02, 2.14), 0.54 (−0.01, 1.66), 0.51 (−0.07, 2.04), 0.56 (−0.08, 2.42), 0.53 (0.04, 1.73) respectively] did not exclude the WBE prediction (a = 1/2) for trees with symmetrical, area-preserving branching, based on large 95% CIs (Fig. 4, Table S5). Further, within each ponderosa pine tree, the observed branch-level values of a_{node} also did not significantly differ from the WBE predicted value based on 95% CIs (Fig. 4).

The observed whole-tree posterior median estimates of a_{tree} were sensitive to the size of the branching network. Values were statistically indistinguishable from the WBE prediction for maple and oak trees and for data sets with minimum tip size > 7 tips for piñon and balsa (Fig. 5a, Table S3). Values of a_{tree} were statistically different from the WBE prediction for ponderosa pine (Fig. 5a, Table S3). Importantly, since area preservation was observed in ponderosa pine trees, deviations from the WBE model prediction indicate asymmetry in branching in this species.

Interspecific patterns. Both the interspecific branch-level [a_{node} = 0.54 (−0.04, 2.01)] and whole-tree [a_{tree} = 0.550–0.591 (0.449, 0.777), range across all subsets] exponent estimates were not significantly different from the WBE prediction of 0.5 (Figs 4 and 5d, Tables S3 and S5).

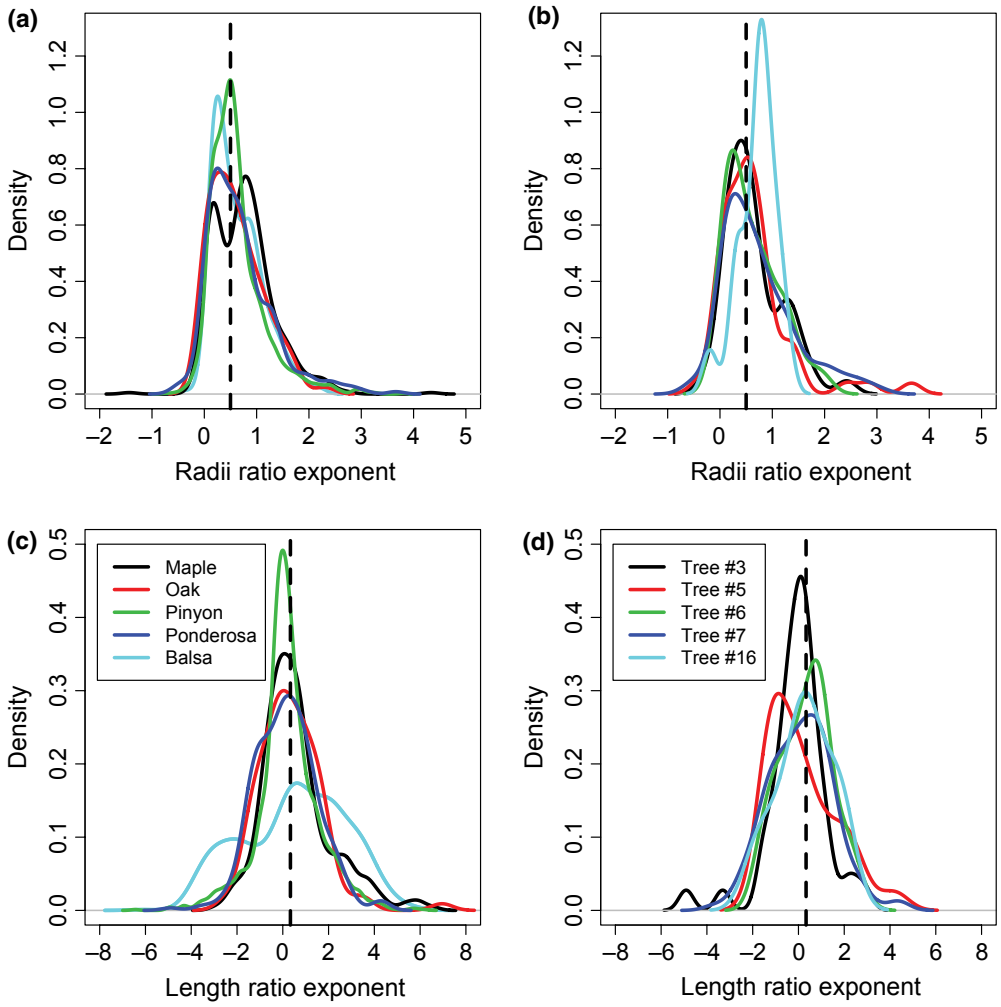

Figure 4 Distributions of branch-level scaling exponents for length (b_{node}) and radii (a_{node}) estimated as kernel density functions using the 'density' function in the statistical platform 'R' (kernel = 'gaussian'). Values of scaling exponents were calculated using the branch-level ratio-based approach for each tree. Data for all ponderosa pine trees were pooled together in the left panels, while the right panels show all individual ponderosa pine trees. The dotted vertical lines indicate WBE predicted values for an idealised tree (a_{node} = 1/2, b_{node} = 1/3).

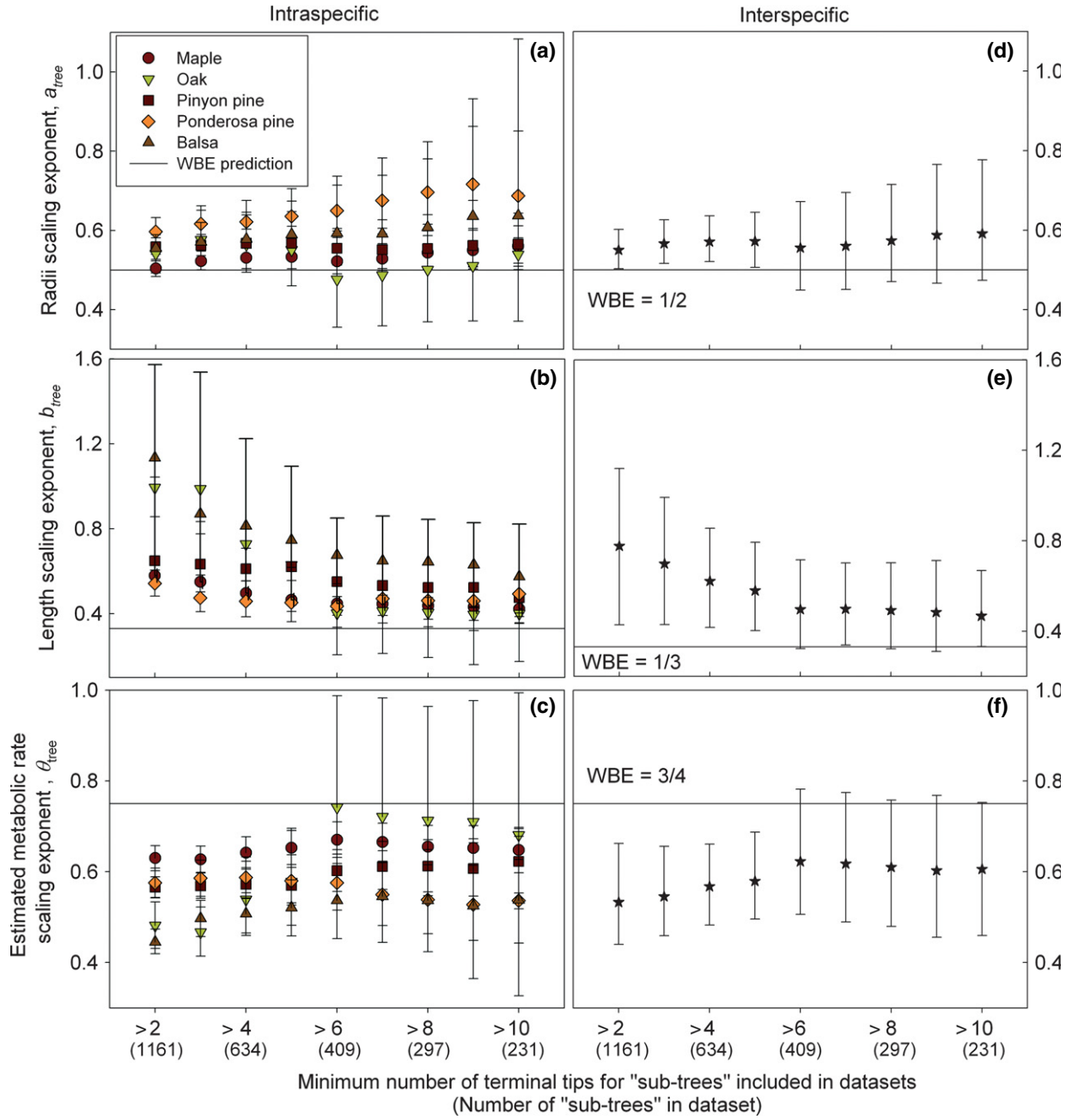

Figure 5 Median and credible intervals (CI) for whole-tree exponents (a_{tree}, b_{tree}, θ_{tree}) estimated within the context of the WBE model using the hierarchical Bayesian analysis. Results are reported for each binned data set (e.g. with a different number of subsets based on the minimum number of tips of a 'sub-tree' included). The WBE prediction for an allometrically optimised plant is indicated by a horizontal solid line.

Do trees exhibit space-filling branching?

Intraspecific patterns. Observed branch-level values of b_{node} for individual species did not exclude the WBE prediction of $b = 1/3$, although large 95% CIs make it difficult to state whether a single narrow prediction or a wide range centred around a predicted value are more appropriate (Fig. 4, Table S5). Interestingly, in concert with the larger range of median values among species for b_{node} (0.13–0.67) compared to a_{node} (0.51–0.72), the variance in b_{node} was also much larger than the observed variance in a_{node} (Fig. 4, Table S5). The greater variability in the distribution of length ratios compared to radii ratios can be further observed by comparing daughter lengths to parent lengths (Fig. 3).

At the whole-tree level, posterior median estimates of b_{tree} were statistically different for maple [b_{tree} = 0.423–0.579 (0.354, 0.627)], piñon [b_{tree} = 0.476–0.650 (0.387, 0.694)], ponderosa [b_{tree} = 0.436–0.53 (0.321, −0.630)] and balsa [b_{tree} = 0.575–1.134 (0.404, 1.223)] trees regardless of subset size (Fig. 5b, Table S3). Posterior median estimates of b_{tree} for oak were not statistically different from the WBE prediction when the minimum number of terminal tips in a subset was > 6 [0.404–0.413 (0.160, 0.623); Fig. 5b, Table S3].

Interspecific patterns. The interspecific branch-level value of b_{node} [0.21 (−3.05, 3.76)] did not exclude the WBE prediction but given extremely large 95% CIs this is not strong support (Fig. 4, Table S5). At the whole-tree level, the interspecific exponent for b_{tree} was significantly greater than the WBE prediction, regardless of data set size [0.467–0.777 (0.310, 1.119); Fig. 5e, Table S3].

Is statistical self-similarity held throughout branching networks within a single tree?

A generalisation of the WBE model is that the average rules for plant architecture are self-similar on average, even if self-similarity does not hold across all nodes. We observed that ratio-based measures of a_{node} and b_{node}, and consequently θ_{node}, do not systematically change with parent diameter (Fig. S1), indicating invariance of these branching traits across branching levels, plant size and taxa.

Do branch- and whole-tree estimates for θ match the WBE prediction of 3/4?

Intraspecific patterns. Although branch-level estimates of θ_{node} across species averaged 0.46 (−5.25, 7.06), they did not exclude the WBE prediction of 3/4 for optimised symmetrically branching trees with no pathlength limitation on hydraulic conductance (Table S5). However, this result is due to very wide density distributions in both a_{node} and b_{node}, which were used to calculate θ_{node} and is also reflected by large 95% CIs for θ_{node} (Fig. 4, Table S5). In contrast, whole-tree architecture-based estimates of θ_{tree} for maple [0.627–0.670 (0.598, 0.710)], piñon [0.566–0.623 (0.532, 0.695)], ponderosa [0.528–0.588 (0.443, 0.639)] and balsa [0.455–0.546 (0.327, 0.678)] trees were statistically less than the WBE prediction for metabolic rate (Fig. 5c, Table S3). Posterior median estimates of θ_{tree} for oak were not statistically different from the WBE prediction when the minimum number of terminal tips in a subset was > 6 [0.681–0.741 (0.519, 0.994); Fig. 5c, Table S3).

Interspecific patterns. The interspecific branch-level value of θ_{node} [0.46 (−5.25, 7.06)] did not exclude the WBE prediction due to large 95% CIs (Table S5). At the whole-tree level, the interspecific exponent for θ_{tree} was significantly less than the WBE prediction, for data sets that included trees with < 6 terminal tips [0.533–0.579 (0.440, 0.687); Fig. 5f, Table S3].

DISCUSSION

Variation in tree branching patterns

Our direct measurements of plant branching architecture from a diverse group of trees lead to calculations of scaling exponents that fall within a relatively narrow range (at least in comparison with the observed range of possible values; Tables S3 and S5). This convergence indicates evolutionary, genetic and/or developmental constraints on similarities in branching architecture and supports plant network models that assume selection on biological networks has resulted in a common set of branching rules (e.g. West *et al.* 1999; Vasseur *et al.* 2012). Nonetheless, some interspecific differences are apparent. For example, in maple, oak and balsa, we observed node-level scaling exponents for branch length that were most similar to each other, while scaling exponents for branch length were consistently different for both ponderosa and piñon pine.

For all species, the scaling of branch radii (represented by a_{node} and a_{tree}) was much less variable than for branch lengths (represented by b_{node} and b_{tree}) (Fig. 4, Table S5). This finding is consistent with other studies examining tree branching architecture where branches tend to be more plastic in terms of their lengths than radius (McMahon & Kronauer 1976; Bertram 1989; Price *et al.* 2007) and studies on asymmetrical branching and tree ontogeny (e.g. Renton *et al.* 2006). These findings are also in concordance with Price *et al.* (2007) who suggested the WBE principle of energy minimisation for water transport leads to minimisation of hydrodynamic resistance. Because resistance depends on radius to the 4th power but only linearly on length, changes in radius lead to much greater changes and penalties in energy minimisation, in turn leading to much stronger stabilising selection on radii than on lengths (Price *et al.* 2010). This flexibility in length scaling will, however, have consequences for the constraint of space-filling branching, which is closely linked with light-gathering in leaves and limbs (Duursma *et al.* 2010; Nishimura *et al.* 2010) and with water/nutrient-gathering in roots (Biondini 2008). Depending on the distribution of lengths within a level and thus the sum total of service volumes for that level, deviations from space filling could be calculated. That is, if enough longer branches are compensated for by smaller branches, a modified version of space filling could still hold throughout the tree even with variation in branch lengths. Similarly, area preservation between mother and daughter branches could still hold with large variation in branch radii.

In addition to large variation in scaling of branch length (b_{node} and b_{tree}), we observed systematic changes in values for scaling exponents dependent on the number of terminal tips per tree included in the analysis (Fig. 5, Table S3). The smaller the number of terminal tips included, the greater the variation (e.g. see error bars Fig. 5). Since we created smaller 'sub-trees' using data from the top of the canopy of whole real trees, these results are consistent with the observation that very young branches near the edges of the canopy have highly variable dimensions, perhaps due to the relaxation of biomechanical constraints (Niklas 1994; West *et al.* 1999) or their active growth. Flexibility is key to peripheral, or sun, branch function. Indeed, studies have found that allometric patterns are different for branches that position leaves to intercept solar radiation (e.g. sun branches) and nearby branches upon which these subordinated sun branches grow (e.g. structural branches, Dahle & Grabosky 2010). This result was most pronounced in the oak tree; a wide range of values (e.g. about a factor 2) for the whole-tree length and estimated metabolic rate exponents were observed, depending on the minimum number of terminal tips (Fig. 2, Table S3).

Testing WBE assumptions and predictions

Although several WBE assumptions and predictions were supported by our results, deviations in scaling of branch lengths (b_{tree}) and estimated metabolic rate (θ_{tree}) from WBE predictions were observed (Fig. 5b, c, Table S3). In particular, all estimates for scaling of branch lengths were significantly closer to 1/2 than the WBE estimate of 1/3. As described above when discussing high variation in estimates of b_{tree}, we hypothesise that considerable differences between individual trees with respect to their principle of crown space filling and the fractal dimension is responsible for this deviation. Indeed, studies have demonstrated a more variable crown scaling than predicted by WBE (Pretzsch & Biber 2005; Pretzsch 2006;

Pretzsch & Dieler 2012). It is also possible that since $b = 1/3$ for whole trees should only occur in large trees (West *et al.* 1999), maximum pathlength by diameter scaling had not yet reached elastic similarity in these relatively young trees (von Allmen *et al.* 2012). From this perspective, future work to improve plant-scaling models should incorporate asymmetrical branching or size dependency resulting from adaptation to physical/environmental conditions and leading plants to diverge from 3D growth patterns.

In addition to deviations in scaling of branch lengths, we also observed branch-level and whole-tree values for the estimated metabolic rate scaling exponent (θ_{node} and θ_{tree}), that were significantly less than the WBE prediction of 3/4 (Fig. 5c, Table S3). While our estimation of metabolic rate scaling was based purely on plant external architecture, θ can also be estimated within the context of WBE by combining structural and physiological trait information. That is, θ can be defined as a composite of how trunk diameter, D, scales with mass, M ($D \propto M^{c}$) and with tree water use ($Q \propto D^{q}$), such that $\theta = c{\cdot}q$ ($Q \propto M^{\theta=cq}$) (Sperry *et al.* 2012). Because our external branching-based analysis does not estimate the water-use exponent q, we assume variation in θ estimates must concern the mass (or volume) scaling exponent, c. The WBE model value for $c = 3/8$ results from assumptions of area-preserving and space-filling branching that leads to a convergence to elastic similarity in large branching networks (Appendix S1).

Our data strongly support area preservation, but failed to support space-filling branching in all trees except the oak (Fig. 5b, Table S3), indicating a potential violation of elastic similarity for most trees studied. Explicit tests of elastic similarity within the same maple and oak trees were evaluated using a log–log plot of each stem diameter against the distance from that diameter to the most distant branch tip. In von Allmen *et al.* (2012), results confirmed these branch networks only converged to elastic similarity with increasing size of larger branches. Smaller branches closer to the tips of the tree were characterised by a steeper scaling of length and diameter than the 2/3-power exponent required for elastic similarity. This well-known shift in branch allometry (McMahon & Kronauer 1976; Bertram 1989; Niklas & Spatz 2004) contributes to the tendency for $c < 3/8$ (and hence $\theta < 0.75$) in data sets such as ours that include smaller branch networks (Sperry *et al.* 2012).

It should also be noted that other studies have shown that smaller trees have exponents for θ that are closer to isometry and across a larger range of sizes, exponents < 1 but $> 3/4$, rather than $< 3/4$ (Reich *et al.* 2006; Mori *et al.* 2010). In these studies, however, metabolic rate was directly measured via respiration and not estimated through plant mass or water-use allometry. Thus, our study highlights a disconnect between theoretical estimates and empirically measured values of θ, perhaps due to differences in the scaling of carbon vs. water.

CONCLUSIONS

Our work shows a degree of convergence in branching patterns across functionally diverse tree species and lends support to several assumptions and predictions of WBE. However, analysis of branching distributions in some trees showed violations of power-law behaviour and rejection of WBE predictions for whole-tree scaling in optimised symmetrically branching trees. To improve the predictive ability of plant-scaling models, future work should focus on (1) measurements of smaller sized branches to identify the underlying sources of variability in tree branching architecture that leads to unimodal and highly variable length distributions; (2) differences in the peaks and widths of the distributions of all scaling exponents to identify different evolutionary and developmental pressures within the context of the WBE core assumption while allowing alternative secondary assumptions for particular taxa and environments; (3) revisions to model theory to account for asymmetrical branching; and (4) exploration of the structural and physiological components of the scaling of metabolic rate ($\theta = c{\cdot}q$) using both theory and empirical data related to both carbon *and* water. Using these approaches to better understand general patterns and variable traits of plant branching networks, we will be able to derive and predict scaling exponents with less uncertainty and thus improve scaling models to represent a broader spectrum of realistic trees.

ACKNOWLEDGEMENTS

We are grateful to William Driscoll, Ashley Wiede, Philippe Gregoire, Vanessa Buzzard, Brad Boyle, Catherine Hulshof, Charles Price, Nathan Swenson, Scott Stark, Evan Sommer, Henry Adams, Maggie Heard, Travis Huxman and B2Earthscience for help with data collection. We appreciate insightful comments of five anonymous referees. We acknowledge hospitality and accommodations of the Santa Fe Institute and Biosphere 2. VMS and JSS acknowledge ARC-NZ Research Network for Vegetation Function (working group 2, vascular design: comparison of theory strands) for their meeting and for initiating their collaboration. L.P.B., V.M.S., B.J.E., D.D.S., E.I.V., J.S.S. and P.B.R. were supported by an NSF ATB Award (0742800). J.C.S. and L.P.B. were supported by NSF Postdoctoral Fellowships in Bioinformatics (DBI-0906005, DBI-0905868). J.S.S. and D.D.S. and E.I.V. were supported by NSF-IBN-0743148.

AUTHORSHIP

LPB, VMS, BJE, JSS and PBR designed the study; LPB, JCS, BJE, DDS, EIV and JSS collected data; LPB and JCS analysed data; LPB wrote the first draft of the manuscript, and all authors contributed substantially to revisions.

REFERENCES

Ackerly, D.D. & Donoghue, M.J. (1998). Leaf size, sapling allometry, and Corner's Rules, phylogeny and correlated evolution in Maples (Acer). *Am. Nat.*, 152, 767–791.

von Allmen, E.I., Sperry, J.S., Smith, D.D., Savage, V.M., Enquist, B.J., Reich, P.B. *et al.* (2012). A species' specific model of the hydraulic and metabolic allometry of trees II: testing predictions of water use and growth scaling in ring- and diffuse-porous species. *Funct. Ecol.*, 26, 1066–1076.

Archibald, S. & Bond, W.J. (2003). Growing tall vs growing wide: tree architecture and allometry of *Acacia karroo* in forest, savanna, and arid environments. *Oikos*, 102, 3–14.

Barker, S.B., Cumming, G. & Horsfield, K. (1973). Quantitative morphometry of the branching structure of trees. *J. Theor. Biol.*, 40, 33–43.

Bertram, J.E.A. (1989). Size-dependent differential scaling in branches: the mechanical design of trees revisited. *Trees*, 4, 241–253.

Biondini, M. (2008). Allometric scaling laws for water uptake by plant roots. *J. Theor. Biol.*, 251, 35–59.

Bosch, J.A., Heo, K., Sliwinski, M.K. & Baum, D.A. (2008). An exploration of LEAFY expression in independent evolutionary origins of rosette flowering in Brassicaceae. *Am. J. Bot.*, 95, 286–293.

Callaway, R.M., DeLucia, E.H. & Schlesinger, W.H. (1994). Biomass allocation of montane and desert ponderosa pine: an analog for response to climate change. *Ecology*, 75, 474–481.

Cannell, M.G.R. (1989). Physiological basis of wood production: a review. *Scand. J. For. Res.*, 4, 459–490.

Costes, E. & Guedon, Y. (2012). Deciphering the ontogeny of a sympodial tree. *Trees Struct. Funct.*, 26, 865–879.

Dahle, G.A. & Grabosky, J.C. (2010). Allometric patterns in *Acer platanoides* (Aceraceae) branches. *Trees Struct. Funct.*, 24, 321–326.

Duursma, R.A., Makela, A., Reid, D.E.B., Jokela, E.J., Porte, A.J. & Roberts, S.D. (2010). Self-shading affects allometric scaling in trees. *Funct. Ecol.*, 24, 723–730.

Eloy, C. (2011). Leonardo's rule, self-similarity, and wind-induced stresses in trees. *Phys. Rev. Lett.*, 107, 258101.

Enquist, B.J., Kerkhoff, A.J., Stark, S.C., Swenson, N.G., McCarthy, M.C. & Price, C.A. (2007). A general integrative model for scaling plant growth, carbon flux, and functional trait spectra. *Nature*, 449, 218–222.

Enquist, B.J., West, G.B. & Brown, J.H. (2009). Extensions and evaluations of a general quantitative theory of forest structure and dynamics. *Proc. Natl Acad. Sci. USA*, 106, 7046–7051.

Feng, L., de Reffye, P., Dreyfus, P. & Auclair, D. (2012). Connecting an architectural plant model to a forest stand dynamics model-application to Austrian black pine stand visualization. *Ann. For. Sci.*, 69, 245–255.

Hallé, F., Oldeman, R.A.A. & Tomlinson, P.B. (1978). *Tropical Trees and Forests: An Architectural Analysis*. Springer-Verlag, New York.

Horn, H.S. (2000). Twigs, trees, and the dynamics of carbon in the landscape. In: *Scaling in Biology* (eds Brown, J.H. & West, G.B.). Oxford University Press, Oxford, pp. 199–220.

Küppers, M. (1989). Ecological significance of above-ground architectural patterns in woody plants: a question of cost-benefit relationships. *TREE*, 4, 375–379.

Leopold, L.B. (1971). Trees and streams: the efficiency of branching patterns. *J. Theor. Biol.*, 31, 339–354.

Leslie, A.B. (2012). Branching habit and the allocation of reproductive resources in conifers. *Ann. Bot.*, 110, 915–921.

Lunn, D.J., Thomas, A., Best, N. & Spiegelhalter, D. (2000). WinBUGS – a Bayesian modelling framework: concepts, structure, and extensibility. *Statist. Comput.*, 10, 325–337.

Makela, A. (2012). On guiding principles for carbon allocation in eco-physiological growth models. *Tree Physiol.*, 32, 644–647.

McMahon, T.A. & Kronauer, R.E. (1976). Tree structures: deducing the principle of mechanical design. *J. Theor. Biol.*, 59, 443–466.

Mori, S., Yamaji, K., Ishida, A., Prokushkin, S.G., Masyagina, O.V., Hagihara, A. *et al.* (2010). Mixed-power scaling of whole-plant respiration from seedlings to giant trees. *Proc. Natl Acad. Sci.*, 107, 1447–1451.

Niklas, K.J. (1994). Size-dependent variations in plant growth rates and the "3/4 – power rule". *Am. J. Bot.*, 81, 134–145.

Niklas, K.J. & Spatz, H.C. (2004). Growth and hydraulic (not mechanical) constraints govern the scaling of tree height and mass. *Proc. Natl Acad. Sci. USA*, 101, 15661–15663.

Nishimura, E., Suzaki, E., Irie, M., Nagashima, H. & Hirose, T. (2010). Architecture and growth of an annual plant *Chenopodium album* in different light climates. *Ecol. Res.*, 25, 383–393.

Olson, M.E., Aguirre-Hernández, R. & Rosell, J.A. (2009). Universal foliage-stem scaling across environments and species in dicot trees: plasticity, biomechanics and Corner's Rules. *Ecol. Lett.*, 12, 210–219.

Pretzsch, H. (2006). Species-specific allometric scaling under self-thinning: evidence from long-term plots in forest stands. *Oecologia*, 146, 572–583.

Pretzsch, H. & Biber, P. (2005). A re-evaluation of Reineke's rule and stand density index. *For. Sci.*, 51, 304–320.

Pretzsch, H. & Dieler, J. (2012). Evidence of variant intra- and interspecific scaling of tree crown structure and relevance for allometric theory. *Oecologia*, 169, 637–649.

Price, C.A. & Weitz, J.S. (2012). Allometric covariation: a hallmark behavior of plants and leaves. *New Phytol.*, 193, 882–889.

Price, C., Enquist, B. & Savage, V. (2007). A general model for allometric covariation in botanical form and function. *Proc. Natl Acad. Sci.*, 104, 13204–13209.

Price, C.A., Ogle, K., White, E.P. & Weitz, J.S. (2009). Evaluating scaling models in biology using hierarchical Bayesian approaches. *Ecol. Lett.*, 12, 641–651.

Price, C.A., Weitz, J.S., Savage, V.M., Stegen, J.C., Clarke, A., Coomes, D.A. *et al.* (2012a). Testing the metabolic theory of ecology. *Ecol. Lett.*, 15, 1465–1474.

R Development Core Team (2012). *R: A Language and Environment for Statistical Computing*. R Foundation for Statistical Computing, Vienna.

Reich, P.B., Tjoelker, M.G., Machado, J.L. & Oleksyn, J. (2006). Universal scaling of respiratory metabolism, size and nitrogen in plants. *Nature*, 439, 457–461.

Renton, M., Guedon, Y., Godin, C. & Costes, E. (2006). Similarities and gradients in growth unit branching patterns during otongeny in 'Fuji' apple trees: a stochastic approach. *J. Exp. Bot.*, 57, 3131–3143.

Rosell, J.A., Olson, M.E., Aguirre-Hernandez, R. & Sanchez-Sesma, F.J. (2012). Ontogenetic modulation of branch size, shape, and biomechanics produces diversity across habitats in the Bursera simaruba clade of tropical trees. *Evol. Dev.*, 14, 437–449.

Savage, V.M., Deeds, E.J. & Fontana, W. (2008). Sizing up allometric scaling theory. *PLoS Comput. Biol.*, 4, e1000171.

Shinozaki, K., Yoda, K., Hozumi, K. & Kira, T. (1964). A quantitative analysis of plant form – the pipe model theory: I. Basic analysis. *Jap. J. Ecol.*, 14, 97–105.

Sone, K., Noguchi, K. & Terashima, I. (2005). Dependency of branch diameter growth in young Acer trees on light availability and shoot elongation. *Tree Physiology*, 25, 39–48.

Sperry, J.S., Smith, D.D., Savage, V.M., Enquist, B.J., McCulloh, K.A., Reich, P.B. *et al.* (2012). A species' specific model of the hydraulic and metabolic allometry of trees I: model description, predictions across functional types, and implications for inter-specific scaling. *Funct. Ecol.*, 26, 1054–1065.

Stegen, J.C., Swenson, N.G., Enquist, B.J., White, E.P., Phillips, O.L., Jorgensen, P.M. *et al.* (2011). Variation in above-ground forest biomass across broad climatic gradients. *Glob. Ecol. Biogeogr.*, 20, 744–754.

Vasseur, F., Violle, C., Enquist, B.J., Granier, C. & Vile, D. (2012). A common genetic basis to the origin of the leaf economics spectrum and metabolic scaling allometry. *Ecol. Lett.*, 15, 1149–1157.

Wang, Y. & Li, J. (2006). Genes controlling plant architecture. *Curr. Opin. Biotechnol.*, 17, 123–129.

Warton, D.I., Wright, I.J., Falster, D.S. & Westoby, M. (2006). Bivariate line-fitting methods for allometry. *Biol. Rev.*, 81, 259–291.

West, G.B., Brown, J.H. & Enquist, B.J. (1997). A general model for the origin of allometric scaling laws in biology. *Science*, 276, 122–126.

West, G.B., Brown, J.H. & Enquist, B.J. (1999). A general model for the structure and allometry of plant vascular systems. *Nature*, 400, 664–667.

West, G.B., Enquist, B.J. & Brown, J.H. (2009). A general quantitative theory of forest structure and dynamics. *Proc. Natl Acad. Sci. USA*, 106, 7040–7045.

SUPPORTING INFORMATION

Additional Supporting Information may be downloaded via the online version of this article at Wiley Online Library (www.ecologyletters.com).

Editor, John Arnone
Manuscript received 13 June 2012
First decision made 24 July 2012
Second decision made 16 November 2012
Third decision made 14 February 2013
Manuscript accepted 22 April 2013